Water Quality Research Journal

Oxygen aeration efficiency of gabion spillway by soft computing models

Rathod Srinivas* and Nand Kumar Tiwari (iD)

Department of Civil Engineering, NIT, Kurukshetra 136 119, India
*Corresponding author. E-mail: rathodsrinivas3252@gmail.com

(iD) NKT, 0000-0002-3153-2531

ABSTRACT

The current paper deals with the performance evaluation of the application of three soft computing algorithms such as adaptive neuro-fuzzy inference system (ANFIS), backpropagation neural network (BPNN), and deep neural network (DNN) in predicting oxygen aeration efficiency (OAE_{20}) of the gabion spillways. Besides, classical equations, namely multivariate linear and nonlinear regressions (MVLR and MVNLR), including previous studies, were also employed in predicting OAE_{20} of the gabion spillways. The analysis of results showed that the DNN demonstrated relatively lower error values (root mean square error, RMSE = 0.03465; mean square error, MSE = 0.00121; mean absolute error, MAE = 0.02721) and the highest value of correlation coefficient, CC = 0.9757, performed the best in predicting OAE_{20} of the gabion spillways; however, other applied models, such as ANFIS, BPNN, MVLR, and MVNLR, were giving comparable results evaluated to statistical appraisal metrics of the relative significance of input parameters based on sensitivity investigation, the porosity (n) of gabion materials was observed to be the most critical parameter, and gabion height (P) had the least impact over OAE_{20} of the spillways.

Key words: adaptive neuro-fuzzy inference systems (ANFIS), backpropagation neural network (BPNN), deep neural network (DNN), dissolved oxygen (DO), gabion spillway, oxygen aeration efficiency (OAE_{20})

HIGHLIGHTS

- An experimental study of the aeration performance of gabion spillways was studied.
- Soft computing techniques have been used to evaluate the aeration performance of the gabion spillways using an experimental dataset.
- DNN was found to be outperforming the model; however, the proposed ANFIS and BPNN models were performing well.
- The sensitivity study suggested that the input parameter, i.e. porosity, was the most sensitive parameter.

GRAPHICAL ABSTRACT
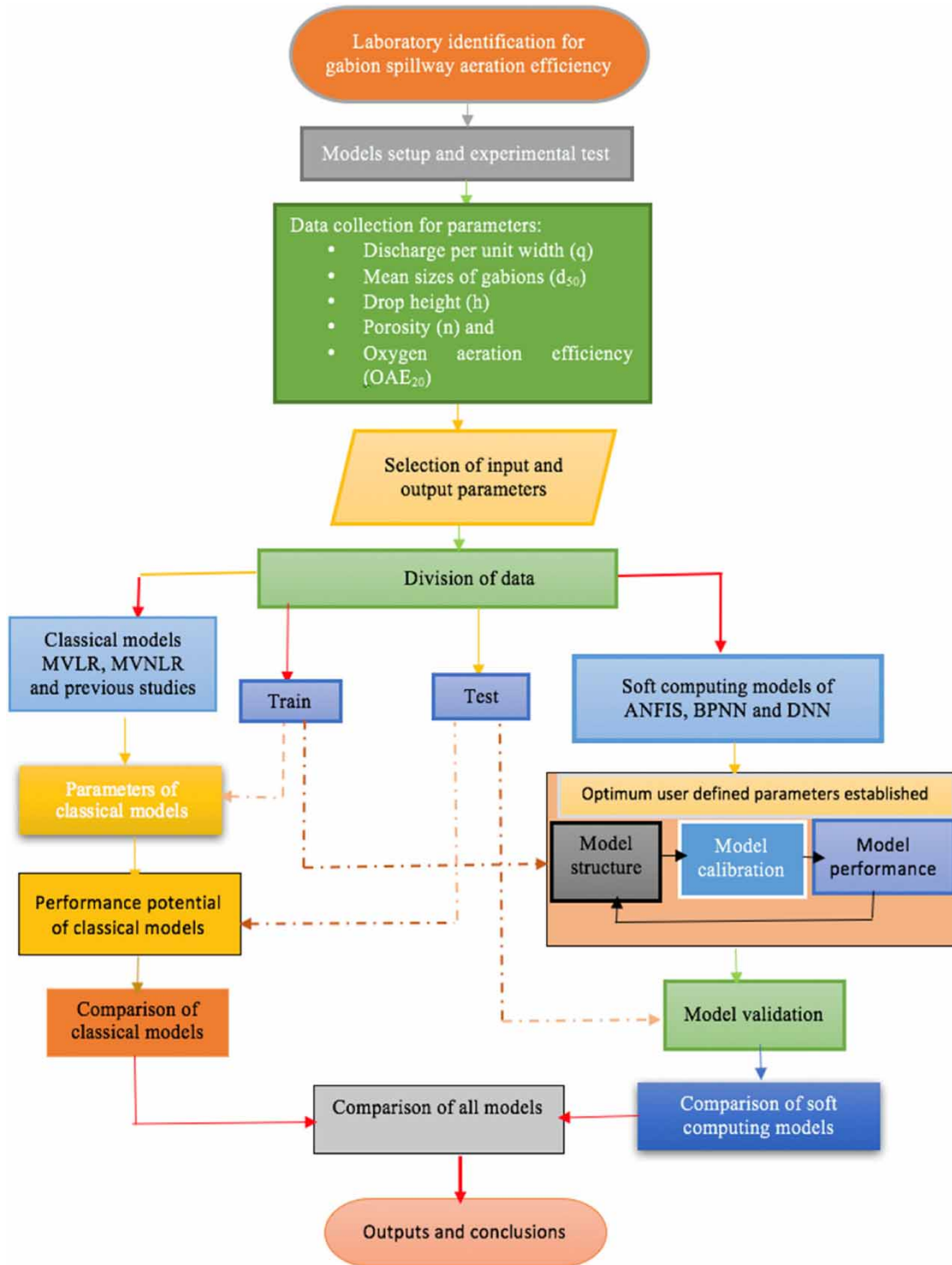
1. INTRODUCTION

The presence of dissolved oxygen (DO) intensity is crucial for the assessment of the health of water bodies. Numerous naturally occurring biological and chemical phenomena consume oxygen present in water, which decrease the amount of DO in

water and increase the strain on aquatic life present in water bodies (Baylar & Emiroglu 2004). Reaeration is the process of enhancing the oxygen in the water by attracting and sucking oxygen from the ambient air; however, aeration is related to the shape, roughness, plunging velocity, and geometry of drop structures of weirs (Luxmi *et al.* 2022). It is possible to enhance aeration by changing the flow form through fluidic structures such as hydraulic jumps and hydraulic drops. These fluidic structures enhance the intensity of DO in rivers, canals, and lakes even if the water will be in contact with the device only for a brief period. The principal cause of this accelerated oxygen transfer is due to the suction and penetration of air into the flow as a result of a huge number of tiny bubbles. These tiny air bubbles enhance the surface area available for oxygen transfer, thereby facilitating larger oxygen exchange (Baylar & Bagatur 2000).

Gabion spillways are frequently used in an earthen dam, the preservation of soil work, retaining structures, river-training work at the bend, and so on. Without the loss of structural integrity, the gabion is stable, flexible, and easy to build. They also withstand considerable differential settlements if any. The gabion structure will be an economical alternative if locally available materials are easily available. It consists of a porous medium filled with different shapes and sizes of coarser materials enclosed by a grid of metal wires. Its porosity helps to drain water which reduces the water load behind the structure. The gabion type of stepped spillways can also be constructed and are commonly used. The flow over the steps also cascades down the spillway face and causes aeration (Salmasi *et al.* 2012). Two types of flow over-stepped spillways are defined by Chanson (2002). They are (a) aerated flow and (b) non-aerated flow. The pressure of water can be reduced by gabions by preserving the permeability and flexibility of rocks (Aal *et al.* 2019). Zhang & Chanson (2016) classified flow over stepped spillways into three hydraulic regimes such as skimming flow, nappe flow, and transition flow. The research concluded that a stepped weir gives good results compared to a flat one (Wuthrich & Chanson 2015). Wormleaton & Soufiani (1998) studied triangular labyrinth weirs and rectangular labyrinth weirs' oxygen aeration potential. In Africa, Sahel gabion spillways are the most normal kind of spillway (Peyras *et al.* 1992). Kells (1994) discussed the dissipation of energy over gabion-stepped weir relating discharge over the crest and critical depth. Chinnarasri *et al.* (2008) studied the characteristics of material present in gabion and also the sensitivity of hydraulic performance experimentally. In addition, the gabion spillway will produce turbulence that will promote aeration and enable the aerobic decomposition of organic matter. It will also help aquatic life to move and migrate more easily (Luxmi *et al.* 2022).

Soft computing data-driven techniques are used for the modeling of oxygen aeration efficiency (OAE) at barrages, spillways, gabion spillways, Parshall flumes, and Montana flumes. They are frequently used due to their accessibility, in-built intelligence, and reliability; besides, they reduce scale effect and avert and avoid model fabrication. So many soft computing techniques have been applied in different domains of water resources and hydraulic engineering. Recently, researchers have shown their interest in using machine learning techniques for predicting the aeration efficiency of gabion weirs with steps and without steps (Luxmi *et al.* 2022; Verma *et al.* 2022). Baylar *et al.* (2011) studied on the prediction of oxygen transfer efficiency in aeration at stepped cascades by using genetic expression programming (GEP) modeling, while Luxmi *et al.* (2022) used gabion weirs where artificial neural network (ANN), Gaussian process regression (GPR), and adaptive neuro-fuzzy inference system (ANFIS) with triangular, trapezoidal, Gaussian, and G-bell membership functions (MFs) used for the estimation of oxygenation, but Verma *et al.* (2022) used stepped gabion weir where oxygen estimation was carried out using ANN and random forest (RF). Modeling and experimental investigation of aeration efficiency at labyrinth weir were carried out by Singh *et al.* (2021). To stimulate the oxygen transfer abilities to plunge jets by utilizing basic flow patterns or flow characteristics and forecast the volume of oxygen transfer coefficient by using modeling techniques such as ANN, adaptive neuro-fuzzy interface system, multivariate adaptive regression splines, multivariate nonlinear regression (MVNLR), and generalized regression neural network (GRNN) were carried out by Kumar *et al.* (2021, 2022).

In the field of scouring, soft computing models were used for the prediction of the scour depth around non-uniformly spaced piles groups by using GPR, RF, and M5 Tree models (Ahmadianfar *et al.* 2021). The assessment of stochastic models for predicting the depth of pipeline scour caused by waves by using the total improvement index was used to compare the performance of the established stochastic models and the genetic programming (GP) method to results achieved using deterministic techniques (Sharafati *et al.* 2018). Besides predicting the depth of scouring at the downstream sluice gate, ANFIS-PSO was used by Sharafati *et al.* (2020b). Modeling of high strength concrete beam for the prediction of shear strength (SS) by the advanced computer aid model of ANFIS, genetic algorithm (GA), differential evolution (DE), ant colony optimizer (ACO), and particle swarm optimization (PSO) attained the best prediction accuracy (Sharafati *et al.* 2020a).

Aeration on spillways is a crucial characteristic related to the strong flow turbulence, free-surface turbulent interactions, and air entrainment. For the drinking water treatment, cascade aeration (stepped spillway-like structure) can be used to

reduce the chlorine content, objectionable taste, and odors. Re-oxygenation cascades were also built downstream of spillways along rivers and canals.

Being porous, organic and dissolved materials can pass through gabion spillways unlike their impervious counterparts, so owing to the least negative impact, gabion spillways are preferred over rigid spillways. Further, gabion spillways have the edge over rigid spillways on account of flexibility, stability, and eco-friendly nature since it permits aquatic life, especially fishes and other small water animals.

The main objective of this current paper was to compare the performance of three soft computing models on the basis of statistical metrics such as the coefficient of correlation (CC), root mean square error (RMSE), mean square error (MSE), and mean absolute error (MAE). Besides, classical equations, namely multivariate linear regression (MVLR) and MVNLR, including previous studies, were also employed in predicting the oxygen aeration efficiency (OAE_{20}) of the gabion spillways. The uniqueness and scope of the work have numerous aspects as the current work summarizes the OAE_{20} by performing the laboratory tests with varying various parameters, including discharge per unit width of the gabion spillway, drop height, gabion spillway means size particle, and porosity. Thereafter, the OAE_{20} was computed and compared with soft computing models, namely, ANFIS, deep neural network (DNN), and backpropagation neural network (BPNN). Sensitivity analysis was also done to get the relative impact of input parameters on the outcomes of the OAE_{20}.

1.1. Background

1.1.1. Oxygen transfer process

A parcel of water that passes through a hydraulic structure (fluidic devices) changes its oxygen intensity over time as it travels through the structure (Lewis & Whitman 1924).

$$\frac{dm}{dt} = V \frac{dI}{dt} = K_L A (I_s - I) \tag{1}$$

where K_L is the coefficient of bulk liquid film for oxygen, I_S is the saturation intensity of DO in water, I is the intensity of DO, A is the area of surface associated with the volume V, over which transfer occurs, t is the time, dm/dt is a rate of the change of mass and dI/dt is a rate of the change in the intensity of dissolved oxygen.

By considering I_S as a constant, the OAE is

$$OAE = \frac{(I_d - I_u)}{(I_s - I_u)} \tag{2}$$

where OAE is the oxygen aeration efficiency, I_d is the intensity of DO at downstream of the fluidic device, I_u is the intensity of DO at upstream of the fluidic device, and I_s is the saturation intensity of DO. When the downstream water is supersaturated ($I_s < I_d$), then OAE > 1. Similarly, when full oxygen transfer reaches the saturation value, then OAE = 1 and OAE = 0 represent no transfer of oxygen.

For comparing results consistently, the OAE is usually normalized to 20 °C. Gulliver *et al.* (1990) presented an equation to illustrate the impact of temperature as

$$(1 - OAE_{20}) = (1 - OAE)^{1/f} \tag{3}$$

The OAE represents the oxygen aeration efficiency at actual water temperature; OAE_{20} represents the oxygen aeration efficiency at 20 °C, and f represents the exponent of the gain described in the following equation:

$$f = 1.0 + 8.26 \times 10^{-5}(T - 20)^2 + 2.1 \times 10^{-2}(T - 20) \tag{4}$$

For hydraulic construction, the overall O_2 transfer may be calibrated by the deficit ratio, 'r', Markofsky & Kobus (1978) described as:

$$r = \frac{I_d - I_u}{I_s - I_d} \tag{5}$$

where I_u is the intensity of DO at the upstream, I_d is the intensity of DO at the downstream, and I_s is the saturation intensity of DO at the equilibrium.

2. MATERIALS AND METHODS

2.1. Proposed modeling techniques

In the current study, modeling of aeration performance of gabion spillways has been investigated by conventional methods, including MVLR, MVNLR, and existing empirical relations and soft computing techniques, namely ANFIS, BPNN, and DNN using an experimental dataset.

2.1.1. Conventional models

In the current study, two regression equations were used to estimate oxygen aeration efficiency (OAE_{20}). One regression equation is MVLR and another one is MVNLR.

The relation between a secondary variable (X) and primary variables (q_1, q_2, q_3, …,) was developed by using a MVLR model or equation. The characteristics layout of the MVLR model is

$$X = p_1q_1 + p_2q_2 + p_3q_3 + \ldots \pm c \qquad (6)$$

in which p_1, p_2, p_3, …, are proportionality constants.

The relation using the MVLR was found to be as follows:

$$OAE_{20} = 0.013q + 0.006P + 0.0065n + 0.0043h - 0.49 \qquad (7)$$

The relation between a secondary variable (X) and primary variables (Z_1, Z_2, Z_3, …,) was developed by using a MVNLR model or equation. The application of a MVNLR model was used for the multiple prediction variables. The characteristics layout of the MVNLR model is

$$X = PZ_1^{K_1}Z_2^{K_2}Z_3^{K_3}, \ldots, Z_n^{K_n} \qquad (8)$$

X is the secondary variable and considered as the output variable; p is the proportionality constant, Z_1, Z_2, …, Z_n are the primary variables and selected as input parameters, and K_1, K_2, K_3, …, K_n are constants of exponential. The relation is found through the MVNLR is as follows:

$$OAE_{20} = 0.0011q^{0.55}P^{0.39}d_{50}^{0.052}n^{0.46}h^{0.35} \qquad (9)$$

In which OAE_{20} is the oxygen aeration efficiency at 20 °C:

$q =$ discharge per unit width in l/s/m (liter/second/meter),
$P =$ height of gabion spillway in cm,
$d_{50} =$ mean size of the materials used in the gabion spillway in cm,
$n =$ porosity in %, and $h =$ drop height in cm.

In the current study, the following models of Luxmi *et al.* (2022) and Tiwari (2021) are mentioned in Equations (10) and (11), respectively, which are used to predict the OAE_{20}.

$$E_{20} = 0.0033Fr^{0.6676}Re^{0.4614} \qquad (10)$$

$$AE_{20} = \left(\frac{d_{50}}{L}\right)^{0.46} n^{0.23}Re^{0.2}Fr^{-0.19} \qquad (11)$$

2.1.2. Adaptive neuro-fuzzy inference system (ANFIS)

ANFIS is a soft computing technique used widely for modeling complex system problems based on input and output parameters (Jang 1993). It is a combination of fuzzy logic and a neural network. There are two types of fuzzy inference

systems (FIS), namely, Mamdani and Sugeno. Sugeno is used very often for mathematical analysis (Tiwari 2021). A schematized structural view is shown in Figure 1(a). Two types of FIS available are grid partitioning and subtractive clustering. Input parameter is related to output by an MF. An MF is a curve that defines how each input point is assigned a membership value between 0 and 1. Input MFs are trimf, trapmf, gaussmf, gbellmf, etc., and the output MFs are linear and constant.

The first-degree Sugeno fuzzy-type comprises four fuzzy sets (if–then), given as

Rule 1: if c is Y_1 and d is Z_1, then

$$f^n_{uu} = n_{11}c + p_{11}d + r_{11} \tag{11a}$$

Rule 2: if c is Y_1 and d is Z_2 then

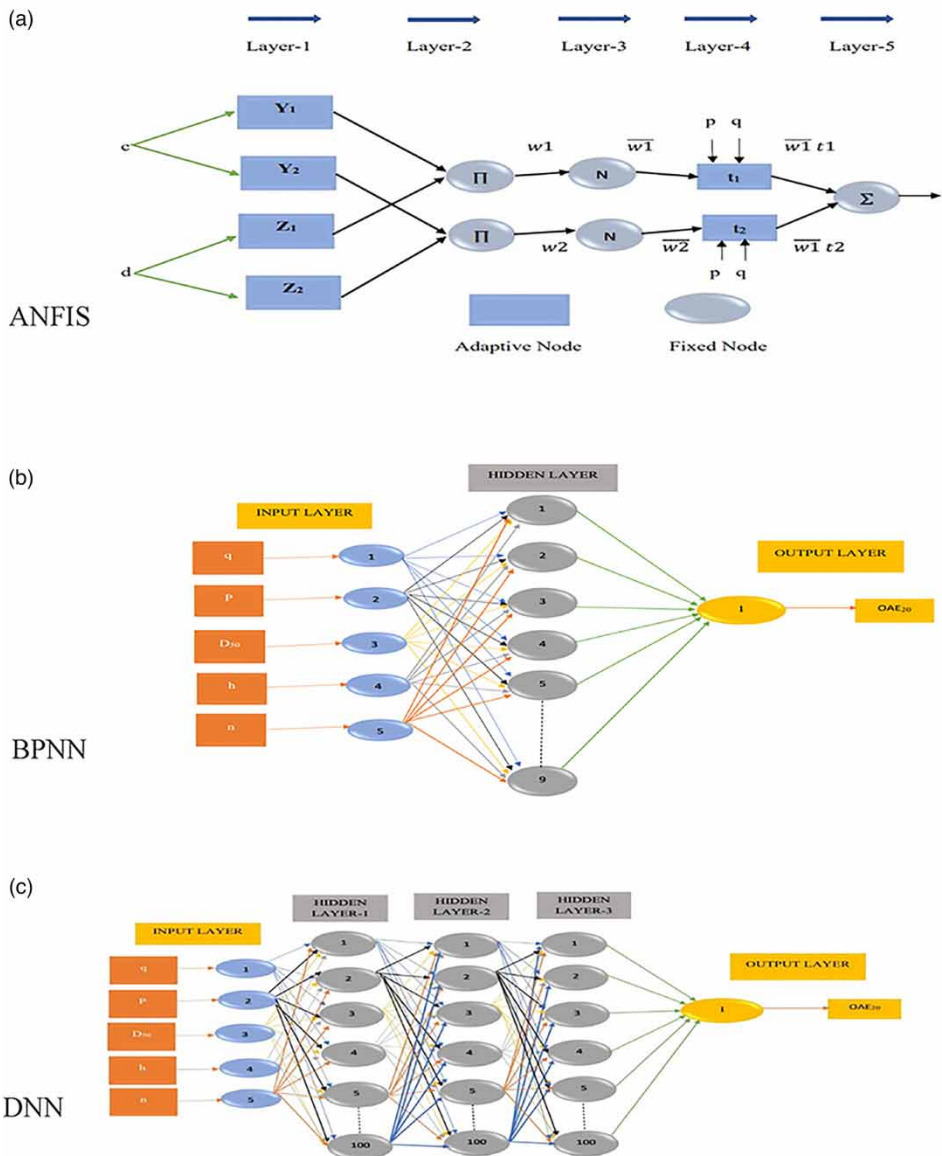$$f^n_{uv} = n_{12}c + p_{12}d + r_{12} \tag{12}$$

Figure 1 | Structures of (a) ANFIS, (b) BPNN, and (c) DNN.

Rule 3: if c is Y_2 and d is Z_1 then

$$f_{uu}^n = n_{21}c + p_{21}d + r_{21} \tag{13}$$

Rule 4: if c is Y_2 and d is Z_2 then,

$$f_{vv}^n = n_{22}c + p_{22}d + ra_{22} \tag{14}$$

where Y_1, Y_2, and Z_1 and Z_2 are fuzzy sets of input c and d f_{uv} $(u, v = 1,2)$

Fuzzification layer (layer 1): every node is an adaptive node and develops membership grade of input and output given by the fuzzification layer, which are:

$$R_{Yc}^1 = \mu_{Yu}(c), \quad u = 1, 2 \tag{15}$$
$$R_{Zd}^1 = \mu_{Zv}(d), \quad v = 1, 2 \tag{16}$$

where c and d are crisp inputs and Y_c and Z_d are fuzzy sets, with low-, medium-, and high-class MF applied, which could take any shape such as triangular function, trapezoidal function, bell-shaped, and Gaussian function.

RULE layer (layer 2): All nodes are fixed and labeled or marked as $\prod$, which play a part of a simple multiplier and outcome given as below:

$$R_{cd}^2 = \omega_{uv} = \mu_{Yu}(c), \quad \mu_{Zv}(d), \quad u, v \ldots = 1, 2 \tag{17}$$

R_{uv}^2 and ω_{uv} are the output of layer 2 and firing strength, respectively.

Normalization layer (average nodes) or layer 3: the role of layer 3 is to normalize the computed firing strengths by dividing each value by the total firing strength as follows:

$$R_{uv}^3 = \omega_{uv} = \frac{\omega_{uv}}{\omega_{11} + \omega_{12} + \omega_{21} + \omega_{22}}, \quad u, v = 1, 2 \tag{18}$$

Defuzzification layer 4 (consequent nodes): the point (node) function of each adaptive point and the output is the yield of standardized firing strength and first-degree polynomial given as follows:

$$R_{uv}^4 = \omega_{uv}t_{uv} = \omega_{uv}(m_{uv}c + n_{uv}d + s_{uv}), \quad u, v \ldots = 1, 2 \tag{19}$$

Output layer 5 (output nodes): the node outcome in the layer is the summation output of the system.

$$R_1^5 = \sum_1^2 \sum_1^2 (\omega_{uv})t_{uv} = \sum_1^2 \sum_1^2 \omega_{uv}(m_{uv}c + n_{uv}d + s_{uv})$$

$$\sum_1^2 \sum_1^2 [\omega_{uv}p)m_{uv} + (\omega_{uv}q)n_{uv} + (\omega_{uv})s_{uv}] \tag{20}$$

2.1.3. BPNN and DNN

The BPNN and the DNN are a subset of machine learning. The BPNN and the DNN consist of neurons similar to the nervous system. Weights and bias are assigned to neurons. These neural networks are designed to perform on the same base as the neurons in the human brain (Fischer 1998). The functioning of a brain neuron involves receiving input and then instigating an output used by another neuron. The neural network security training also works on a similar pattern. They stimulate behavior by learning about the collected data and then predicting outcomes (Nigrin 1993). The BPNN carries out by employing a massive number of highly interconnected nodes (neurons) that work to solve specific problems such as forecast and pattern classification (Bishop 1995). BPNN is widely used to solve water resources problems, and it is a prevalent soft

computing technique. BPNN and DNN include an input layer, the hidden layer, and the output layer. The primary difference between BPNN and DNN is that several hidden layers are present, as well as several nodes in the DNN are present in comparison to the BPNN. In the case of conventional BPNN, only one hidden layer is present, and in DNN, the number of hidden layers is more than one. That is why the DNN is called a deep neural network. The current study model of BPNN was developed using WEEKA software, and the model of DNN was developed using H_2O software. The structure of BPNN and the DNN are shown, respectively, in Figure 1(b) and 1(c).

2.2. Experimental program

The experiments were conducted in the water resource laboratory of the Civil Engineering Department, National Institute of Technology, Kurukshetra. A rectangular rigid steel flume with a width of 25 cm, a height of 30 cm, and a span of 4 m was installed. The flume had a 1.8-m-long transparent acrylic sheet in the mid-section on both sides of the walls. The channel was fitted with a 2HP motor pump that could offer a maximum outflow (discharge) of 5.2 l/s. A re-circulated closed system was developed in the flume, which regularly feeds the channel by redrawing water from a storage cum aeration rectangular tank having overall sizes of 87-cm long, 87-cm wide, and 90-cm in depth. The digital flow meter was used to measure the rate of flow. The model was installed at the downstream end of the channel. The water depth in the channel was measured using a pointer gauge. By mixing the calibrated amount of chemicals, cobalt chlorides, and sodium sulfites, it was possible to reduce the DO in the water to 1–2 mg/l (Emiroglu & Baylar 2003; Tiwari & Sihag 2020; Tiwari 2021). From the chemical mixing tank, water enters the channel through the headbox containing a screen, which dampens the flow and reduces eddies. The water inflow was controlled by a regulating valve fitted in the pipe, as shown in Figure 2. Using the azide modification method (APHA and WEF 2005), DO was measured where the temperature of the water was measured by using a manual thermometer with a precision of 0.5 °C in a range of −10 to 50 °C (Raikar & Kamatagi 2015). Configuration and dimension of all the four-exchangeable spillway models are shown in Table 1. During the experimentation, models were installed with a proper fixing arrangement at the d/s end of the channel gabion spillway. Each gabion spillway was tested under a flow rate varying from 0.5 to 5 l/s. The depth of the waterfall over the gabion spillway's crest to the storage tank's top level is denoted by the drop height (h). It varied in the range of 48–93.4 cm.
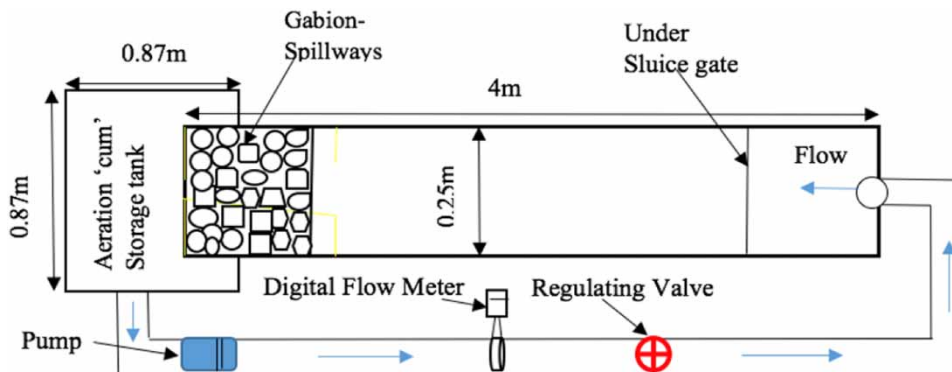

Figure 2 | Schematized top view.

Table 1 | Configuration of models

S. No.	Model	Description	Size of the model (cm)	Gabion size d_{50} (mm)	Porosity (n) %
I	Impervious model	Spillway without step	$40 \times 25 \times 20$	–	–
II	Pervious model	Gabion spillway without step	$40 \times 25 \times 20$	7.86, 26.4, 29.4, and 49.20	24.7, 34,44, and 57
III	Pervious model	Gabion spillway, with one step	$40 \times 25 \times 20$	7.86, 26.4, 29.4, and 49.20	24.7, 34,44, and 57
IV	Pervious model	Gabion spillway with two steps	$40 \times 25 \times 20$	7.86, 26.4, 29.4, and 49.20	24.7, 34,44, and 57

2.2.1. Methodology

The experimental procedure was started after deoxygenating the aeration cum storage tank water to a level between 1 and 2 mg/l by adding an appropriate quantity of sodium sulfite (Na_2SO_3) and cobalt chloride ($COCl_2$). A sample from the deoxygenated water in the tank was withdrawn for the measurement of DO, which represents the initial DO value (upstream DO intensity, I_u). After 85 s (1.25 min) of running the flume (Kumar $et\ al.$ 2021), another sample containing the oxygenated water was drawn from the tank for the final DO measurement (downstream DO Intensity, I_d) after aeration. The azide modification method (APHA and WEF 2005) was used to measure the DO values of the samples. By utilizing Equations (2)–(4), the OAE_{20} was computed. The method was continued for several runs of observations by using one classical impermeable spillway and three pervious gabion spillways also with varying drop heights, and thus, 161 observations of the OAE_{20} were collected.

3. MODEL PERFORMANCE METRICS

The model performance metrics of proposed models were analyzed by statistical measures, i.e., the CC and RMSE, MSE, and MAE.

Correlation of coefficient (CC): the mathematical equation of CC can be expressed as:

$$CC = \frac{N \sum_{i=1}^{N} OAE_{20_{obs}} OAE_{20_{pre}} - \left(\sum_{i=1}^{N} OAE_{20_{obs}}\right)\left(\left(\sum_{i=1}^{N} OAE_{20_{pre}}\right)\right)}{\sqrt{\left[N\left(\sum_{i=1}^{N} OAE_{20_{obs}}^2\right) - \left(\sum_{i=1}^{N} OAE_{20_{obs}}\right)^2\right]\left[N\left(\sum_{i=1}^{N} OAE_{20_{pre}}^2\right) - N\left(\sum_{i=1}^{N} OAE_{20_{pre}}\right)^2\right]}} \tag{21}$$

RMSE: the formula OR equation of the RMSE can be expressed as:

$$RMSE = \sqrt{\frac{1}{N}\sum_{i=1}^{N}(OAE_{20_{obs}} - OAE_{20_{pre}})^2} \tag{22}$$

MSE: the MSE equation can be represented as the following relation given as follows:

$$MSE = \frac{1}{N}\sum_{i=1}^{N}(OAE_{20_{obs}} - OAE_{20_{pre}})^2 \tag{23}$$

MAE: the equation of the MAE is given in the following relation:

$$MAE = \frac{1}{N}\sum_{i=1}^{N}|OAE_{20_{obs}} - OAE_{20_{pre}}| \tag{24}$$

where $OAE_{20_{obs}}$ is the observed OAE at 20 °C, $OAE_{20_{pre}}$ is the predicted OAE at 20 °C, and N is the total number of observations.

3.1. Dataset

A total of 161 experimental readings were utilized for making the model. The input datasets comprise of discharge-per-unit width (q), mean sizes of gabions (d_{50}), drop height (h), gabion spillways height (P), porosity (n), and output data is the oxygen aeration efficiency (OAE_{20}). For training, 75% of the total data were taken, and the net left out 25% of the total datasets were utilized for testing. The statistical summary details of training and testing are shown in Table 2.

4. RESULTS AND DISCUSSION

The dataset was obtained from experimental observations, and the proposed conventional methods of MVLR, MVNLR, existing predictive equations, and soft computing techniques such as ANFIS, BPNN, and DNN were utilized as modeling

Table 2 | Statistical summary for training and testing data

Variables	Units	Min.	Max.	Mean	Std.
	Training data				
q	l/s/m	2	20.4	12.786	5.968
P	cm	10	20	18.032	3.833
d_{50}	cm	0	5.3	3.410	1.885
n	%	0	57	39.772	11.491
h	cm	46.89	93.4	68.108	11.621
E_{20}	–	0.013	0.559	0.340	0.1149
	Testing data				
q	l/s/m	2	20.4	12.786	5.968
P	cm	10	20	18.032	3.833
d_{50}	cm	0	5.3	3.410	1.885
n	%	0	57	39.772	11.491
h	cm	46.89	93.4	68.108	11.621
E_{20}	-	0.013	0.559	0.340	0.1149

techniques. In the current study, a total of 161 observed datasets were taken. The observed datasets were randomly divided into two groups, one was for training data (121 data) and another was for testing data (40 data).

4.1. Results of the ANFIS model

In the current study, the ANFIS model was developed by using MATLAB software. It is a Sugeno and Takagi fuzzy-type approach. By trial-and-error methods, the development of the ANFIS model was carried out. Many models were tried for prediction by the ANFIS model using grid partition. Grid partition subdivides input MFs like trapezoidal MF (trapmf), triangular MF (trimf), generalized membership bell-shaped function (gbellmf), the difference between two sigmoids MF (dsigmf), the product of two sigmoid MF (psigmf), Gaussian2 MF (gauss2mf), Gaussian MF (gaussmf), and pie-shaped MF (pimf) were used for the input MF in the ANFIS model. To train, the FIS hybrid optimization method was used in the model with a zero-error tolerance and epochs of 20. The rule of the model is formed by the 'AND' logical Operation. The output MF was used as a 'constant' for the ANFIS model. Among the all-input-type MF (input MFs type), the pie-shaped MF (pimf) was found to be performing well, while other shaped MFs were performing very poorly and neglected. The agreement diagram between observed values of the OAE_{20} of the gabion spillways and the corresponding predicted values by Pie-shaped MF-based ANFIS is shown in Figure 3 for both the training and testing datasets. This figure suggests that predicted testing points of the OAE_{20} lie around the ideal line, but its training values lie closer to the perfect line and the reason attributed was that CC (0.9571) was high in training in comparison to testing (CC = 0.8799). This fact was further buttressed by closely observing Table 3, where the error values were relatively less in training in comparison to the testing and could be used for forecasting the OAE_{20} of the gabion spillways.

4.2. Results of BPNN

In the current study or work, for estimating oxygen aeration efficiency (OAE_{20}), the BPNN approach was considered in forecasting the model. The BPNN consists of a manifold layer and every layer has nodes (neurons). The layer is joined with a weighted connection (coefficients of weights). Usually, three categories of the layer are formed in the ANN: the first layer signifies (signal) input, the hidden (middle) layer for evaluating input weights, and the output layer is the final layer. The BPNN was established in three stages. In the initial stage, training data were prepared; in the second stage, various positioning and assembled of effective network architectures were needed; and in the final stage, testing (validating) was performed. The number of neurons in hidden layers is selected using trial-and–hit methods. The optimum value of neurons in the hidden layer was observed to be 9, and one hidden layer was performing well. Similarly, the established tuning learning rate, momentum, and number of iterations (epochs) which were giving closed to desired results which were 0.4, 0.3, and 500, respectively.
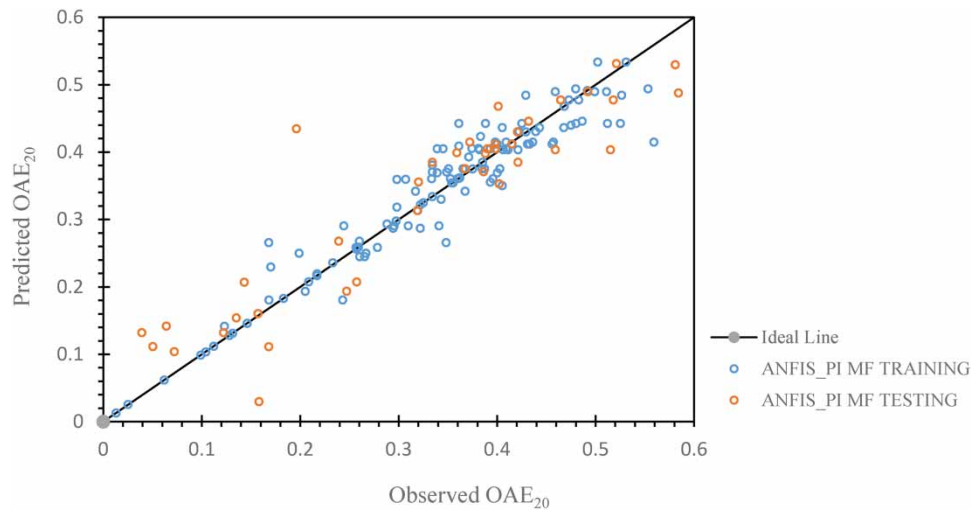
Figure 3 | Performance of ANFIS for training and testing data patterns.

Table 3 | Performance evaluation with proposed techniques

Proposed approaches	CC	RMSE	MSE	MAE
	Training data			
Tiwari (2021)	0.9820	0.36095	0.13028	0.34183
Luxmi *et al.* (2022)	0.5221	0.56984	0.32470	0.52700
MVLR	0.9058	0.04924	0.00242	0.04043
MVNLR	0.8531	0.06159	0.00379	0.04818
ANFIS_PIMF	0.9571	0.03368	0.00113	0.02265
BPNN	0.9456	0.03790	0.00143	0.03031
DNN	0.9763	0.02584	0.00066	0.01987
	Testing data			
Tiwari (2021)	0.9850	0.35475	0.12584	0.30204
Luxmi *et al.* (2022)	0.44771	0.55178	0.30448	0.51270
MVLR	0.8881	0.07278	0.00529	0.04885
MVNLR	0.9028	0.06625	0.00438	0.05348
ANFIS_PIMF	0.8799	0.07514	0.00564	0.04975
BPNN	0.9031	0.07282	0.00612	0.06700
DNN	0.9757	0.03465	0.00121	0.02721

Figure 4 depicts the BPNN-based model scattered plot between observed OAE_{20} and its predicted values for both training and testing datasets. It was observed that barring some predicted points for testing datasets, all predicted points were lying near the ideal line. Further, by observing Table 3, it was shown that BPNN was performing well and could be used in the prediction of OAE_{20} for the gabion spillway as the value of CC is higher and error values are smaller.

4.3. Results of the DNN model

The DNN model was developed by using free auto-machine learning H_2O software. Many models were developed by changing the percentage of the division of training data (calibrating data) and testing data (validating data). A total number of 161 datasets were used for modeling. Finally, 75% of training data (121) and 25% of testing data (40) were found suitable for the
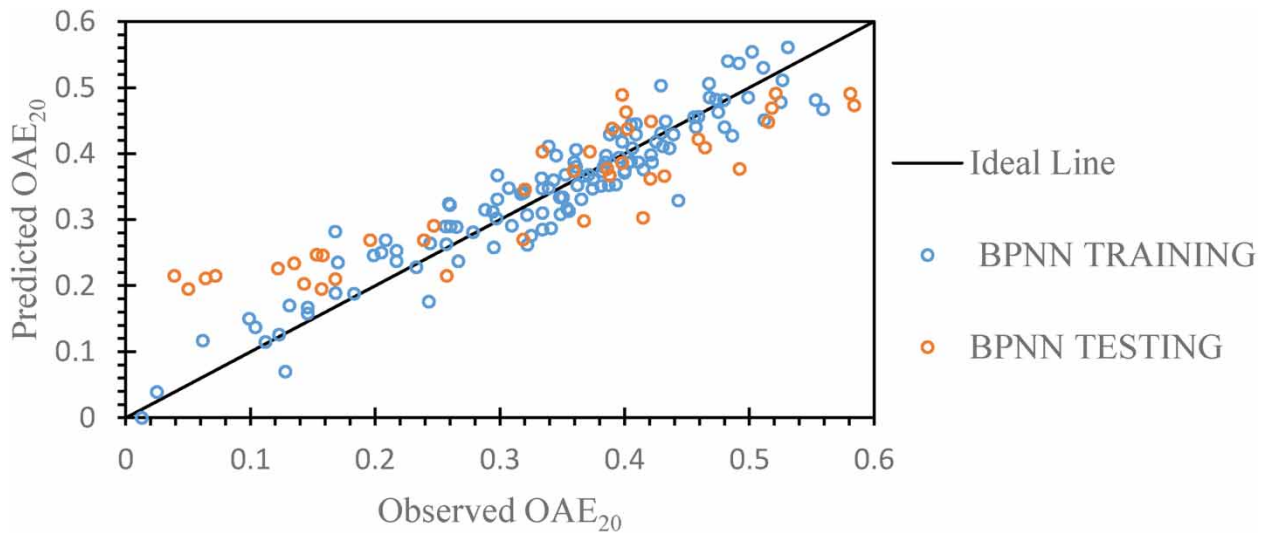
Figure 4 | Performance of BPNN for training and testing data patterns.

prediction of the best model. In a DNN, the initial stage was to be found the number of epochs. These were essential in forecasting the accurate values by considering minimum reckoning cost. The dataset of calibrating (training) was split into five-folds. Each fold was composed of 25 datasets, and the testing (validating) dataset was also divided into five-folds, and each fold was made up of eight datasets. The trial-and-error techniques were used for tuning the principal parameters where the optimized number of folds was found as a 5, and the number of hidden layers was recorded as a 3, each with 100 nodes. The activation function as a rectifier with dropout and the Gaussian distribution function were employed where optimized values of epoch and rho were found as 2,100 and 0.95, respectively. Besides, three hidden dropouts having a value of 0.1 were used.

Figure 5(a) represents the variation in the deviation of the outcomes for training (calibrating) and testing (validating) datasets versus the epochs, and when it was carefully noticed, then it was found that when the value of epochs tends to 2,100, the deviation acquired asymptotic to the abscissa. Further, Figure 5(b) shows the scatter plot between observed and predicted oxygen aeration efficiency (OAE_{20}) by DNN of the gabion spillways for training and testing datasets. Figure 5(b) demonstrates that all predicted values, either in testing or training, were lying along the ideal line, which implied that the DNN is the most performing model. This observation was further substantiated by observing Table 3, where the value of CC was the highest and error values were the lowest among all the proposed models.

4.4. Results of MVLR, MVNLR, and conventional models

The MVLR and MVNLR models were developed by using XLSTAT software which is shown in Equations (7) and (9), and from Figure 6, which is an agreement diagram between the results of MVLR and MVNLR, Luxmi *et al.* (2022) and Tiwari (2021) observed the values of the OAE_{20} for training and testing datasets. From Figure 7, it was observed that MVLR and MVNLR have shown the best results compared to Luxmi *et al.* (2022) and Tiwari (2021) as predicted points by MVLR and MVNLR lie near the ideal line, while Luxmi *et al.*'s (2022) model was overestimated as predicted data points lie above the ideal line, and Tiwari's (2021) model was underestimated as predicted data points lie below the ideal line. In corroboration with the results in Table 3, it can be shown that error values for both MVLR and MVNLR models have less error in comparison to model results found by Luxmi *et al.* (2022) and Tiwari (2021). However, the MVNLR model with a higher value of CC = 0.9228 and lower values of RMSE = 0.06625, MSE = 0.00438, and MAE = 0.05348 were performing better than MVLR with CC = 0.8881, RMSE = 0.0727, MSE = 0.00529, and MAE = 0.04885 for the test datasets.

4.5. Comparison of results

The models developed using datasets of gabion spillways were compared using appraisal parameters as shown in Table 3. All the models, namely MVLR, MVNLR, ANFIS, BPNN, and DNN models, were efficient in making predictions of the OAE_{20} of
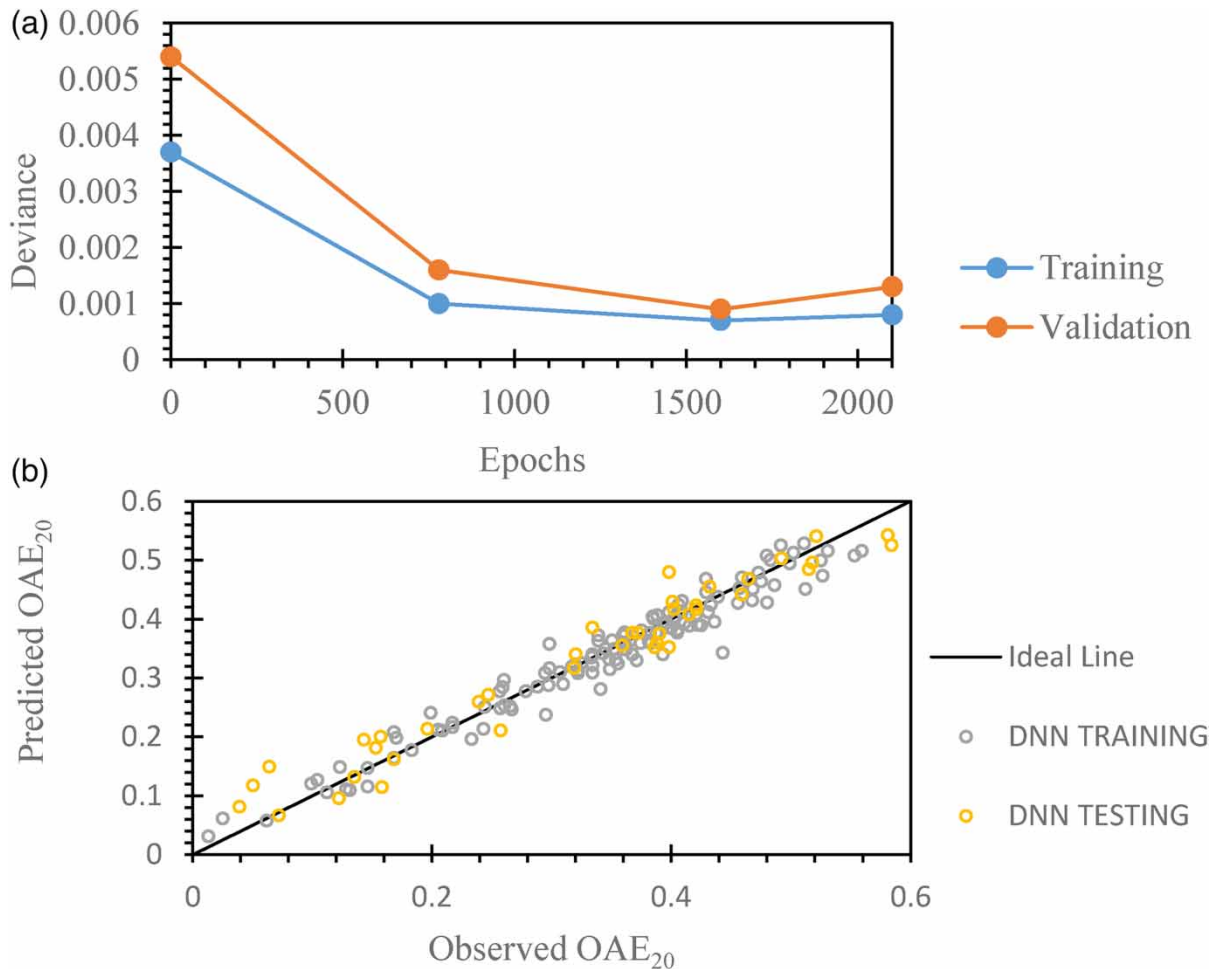
Figure 5 | (a) Scoring deviance and (b) performance of DNN.

the gabion spillways. However, the DNN model outperformed all the proposed models in predicting the OAE of the gabion spillways as the DNN model had the highest CC value and lowest error values, as shown in Table 3 for both the training and testing datasets. All proposed soft computing models were performing better than conventional models in training, but in the case of testing, MVNLR was performing comparably to ANFIS for the present datasets.

Further, Figure 7(a) presents an agreement diagram between the observed and predicted values of the gabion spillways' OAE using soft computing models: ANFIS_PI MF, BPNN, and DNN. It could be observed from Figure 7(a) that, by and large, the majority of predicted results for the OAE_{20} fell around the ideal line. Four more error lines in the domain of ± 25 and $\pm 15\%$ were also drawn between the predicted and observed values of the OAE_{20} of the gabion spillways. Figure 7(a) shows that most of the predicted values of the OAE_{20} by BPNN and DNN were lying well within the $\pm 15\%$ error line from the perfect agreement line in both training and testing cases, but some values of the ANFIS_PI MF model were lying beyond the $\pm 25\%$. So, barring some predicted points, all predicted values by the soft computing algorithms lie in the range of $\pm 25\%$ error lines for the training and testing datasets. Further, there could be drawn an inference from Figure 7(a) that for dimensionless datasets, DNN and BPNN were performing well as their predicted points lie within the $\pm 15\%$ error band for both training and testing datasets; however, all other considered machine learning models gave values which lie in the range of $\pm 25\%$ error band. The above observation is consistent with Figure 7(b), where it was shown that predicted values by the DNN model were lying close to the observed values, which were followed by BPNN and ANFIS_PI MF models. There has been observed a poor performance of conventional models. The summary statistics of predicted results by all proposed models are presented in Table 4 for the training and testing datasets.
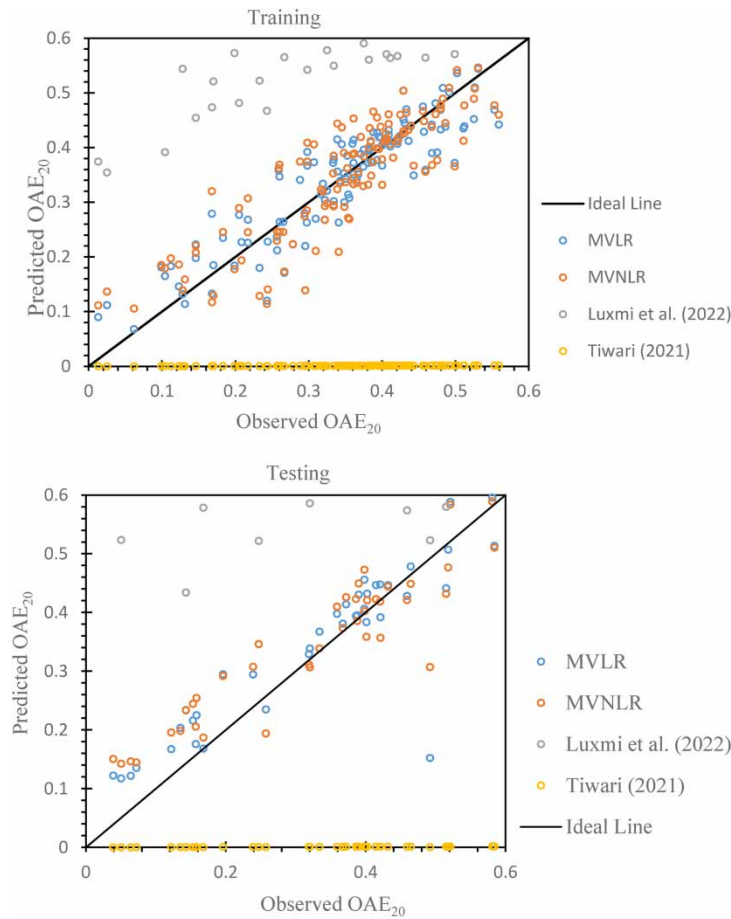
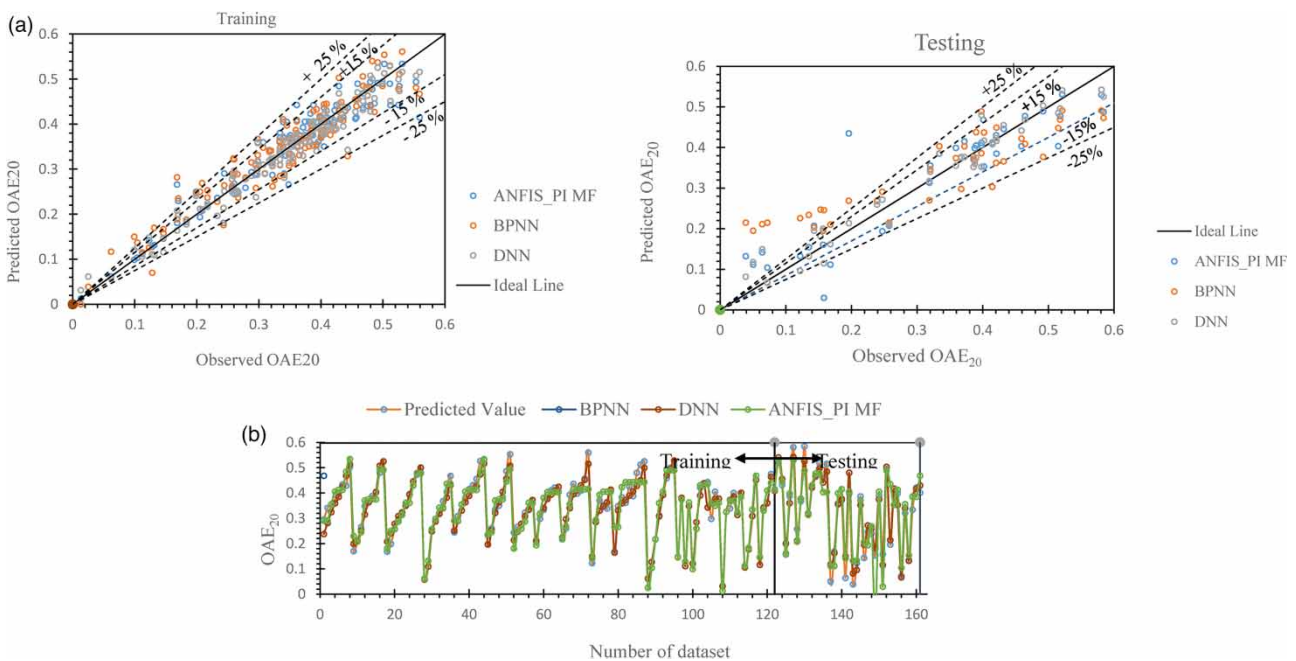**Figure 6** | Performance of MVLR, MVNLR, and other conventional models.

Figure 7 | (a) Performance for the training and testing phases, and (b) observed OAE_{20} and predicted OAE_{20} with several datasets.

Table 4 | Summary details of predicted values

Models	Min.	Max.	Mean	Std.
	Training data			
Actual	0.013	0.559	0.3400	0.1203
Tiwari (2021)	0.354	1.334	0.863	0.2652
Luxmi et al. (2022)	0.002	0.0001	0.001	0.0003
MVLR	0.068	0.544	0.3300	0.1098
MVNLR	0.1056	0.5464	0.3301	0.1143
DNN	0.0313	0.5284	0.3345	0.1150
ANFIS_PIMF	0.013	0.5338	0.3400	0.1150
BPNN	0	0.561	0.3428	0.1140
	Testing data			
Actual	0.039	0.5840	0.3135	0.1606
Tiwari (2021)	0.00018173	0.0018	0.0009	0.0005
Luxmi et al. (2022)	0.4340	1.3249	0.81378	0.25560
MVLR	0.1175	0.5959	0.3322	0.1421
MVNLR	0.1425	0.5892	0.3349	0.1309
DNN	0.0668	0.5426	0.3189	0.1504
ANFIS_PIMF	−0.1170	0.5313	0.3122	0.1619
BPNN	0.195	0.491	0.3305	0.1121
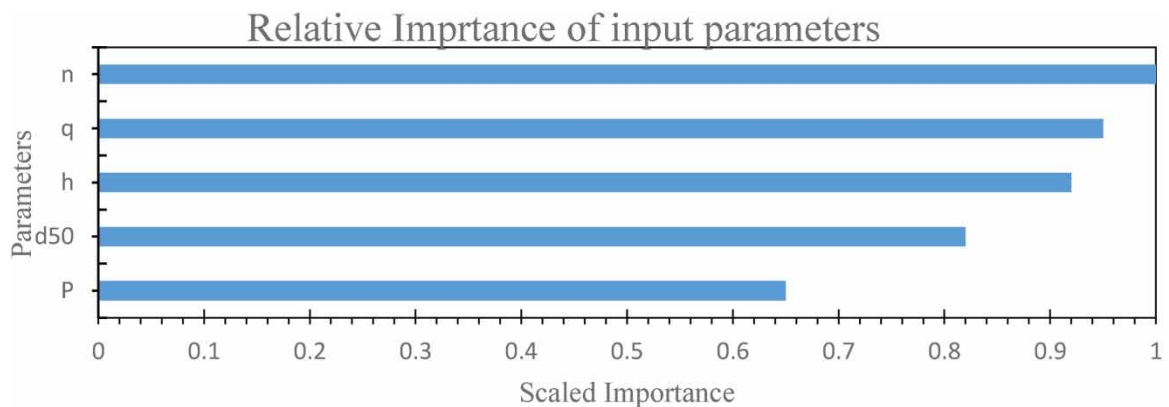
Figure 8 | Sensitivity study of input parameter.

The poor performance of conventional models compared to the proposed soft computing techniques was attributed to the fact that these models could not have the potential to consider all aspects responsible for a complex nonlinear phenomenon that took place during the aeration process at the gabion spillway. In contrast, soft computing approaches are data-driven techniques. They do not require any restrictive assumptions on the form of the model, besides the fact that they can generalize and detect complex nonlinear relationships between dependent and independent variables.

4.6. Sensitivity study

A sensitivity analysis was carried out to determine the relative importance of the independent input parameters. Figure 8 depicts a graph between input parameters versus scale importance using the best-performing DNN model. The most sensitive

parameter was found to be porosity (n) of the gabion material as it read out a maximum of 1 on the scale importance. However, the gabion spillway height (P) was the least sensitive parameter since it read out a minimum of 0.65 on scale importance.

5. CONCLUSIONS

In the current study, modeling of aeration performance of gabion spillways was investigated by conventional methods, including MVLR and MVNLR, considered existing empirical relations, and proposed soft computing techniques, such as ANFIS, BPNN, and DNN using an experimental dataset. From the above works, the following key conclusions were drawn:

1. The performance evaluation of the three soft computing techniques was carried out based on the CC, RMSE, MSE, and MAE. These three soft computing techniques' models utilized experimental datasets to predict the OAE_{20} of the gabion spillways. Out of these three soft computing models, it was observed that the DNN model was found to be the best-performing one in both training and testing as the highest values of CC = 0.9763, and lowest values of RMSE = 0.02584, MSE = 0.00066, and MAE = 0.01987 for the training and the highest value of CC = 0.9757, and the lowest values of RMSE = 0.03465, MSE = 0.00121, and MAE = 0.02721 for the testing in comparison to other models.
2. This study further showed that the BPNN model had an adequate potential for predicting gabion spillway OAE and was the second-best performing model after the DNN, in which the number of neurons in the hidden layer was found to be more sensitive, and its optimum value was nine.
3. The ANFIS_ PI MF model could be used to predict the OAE_{20} of the gabion spillways but was found to be the least-performing model in comparison with the other proposed soft computing models.
4. Both MVNLR and MVLR models were also performing well, but MVNLR performed better than MVLR in predicting gabion spillway OAE, as compared to other results found in the literature.
5. The sensitivity study suggested that the porosity of the gabion spillways material was the most sensitive parameter, while the geometry height of the gabion spillways was the least sensitive parameter.

The experimental test limitation is that water remains in contact not only in models where air mixing occurs due to gravity but also throughout with the flume length. It is attributed because the flow in the flume is always under gravity. Further, soft computing techniques are data-driven and depend on the volume and quality of the dataset. So, another limitation is its comparatively small size and the limited range of experimental datasets.

Future studies could extend these findings by using a more extensive dataset from the laboratory or field to investigate whether better predictions can be achieved for arriving at more specific conclusions. Besides, some other soft computing techniques, namely, support vector method, RF, M5 Model tree, and hybrid soft computing techniques (ANFIS-PSO, ANFIS-GA, etc.), may be tried to compare the results.

AUTHOR CONTRIBUTIONS

R.S. and N.K.T. conceptualized the article, conducted formal analysis, and investigated the article. R.S. wrote the original draft preparation. N.K.T. wrote the review, edited the article, and supervised the work.

DATA AVAILABILITY STATEMENT

Data cannot be made publicly available; readers should contact the corresponding author for details.

CONFLICT OF INTEREST

The authors declare there is no conflict.

REFERENCES

Aal, G. M. A., Fahmy, M. R., Elznikhely, E. A. & El-Tohamy, E. 2019 Energy dissipation and discharge coefficient over stepped gabion and buttress gabion spillway. *Technology* **10** (4), 260–267.

Ahmadianfar, I., Jamei, M., Karbasi, M., Sharafati, A. & Gharabaghi, B. 2021 A novel boosting ensemble committee-based model for local scour depth around non-uniformly spaced pile groups. *Engineering with Computers* 1–23. https://doi.org/10.1080/1064119X.2019.1676335.

APHA and WEF. 2005 *Standard Methods for the Examination of Water and Wastewater*. American Public Health Association/American Water Works Association/Water Environment Federation, Washington DC. vol. 21, pp. 258–259

Baylar, A. & Bagatur, T. 2000 Aeration performance of weirs. *Water SA* **26** (4), 521–526.

Baylar, A. & Emiroglu, M. E. 2004 An experimental study of air entrainment and oxygen transfer at a water jet from a nozzle with air holes. *Water Environment Research* **76** (3), 231–237.

Baylar, A., Unsal, M. & Ozkan, F. 2011 GEP modeling of oxygen transfer efficiency prediction in aeration cascades. *KSCE Journal of Civil Engineering* **15** (5), 799–804.

Bishop, C. M. 1995 *Neural Networks for Pattern Recognition*. Oxford University Press, Birmingham, UK.

Chanson, H. 2002 *Hydraulics of Stepped Chutes and Spillways*. CRC Press. The University of Queensland Brisbane, Australia.

Chinnarasri, C., Donjadee, S. & Israngkura, U. 2008 Hydraulic characteristics of gabion-stepped weirs. *Journal of Hydraulic Engineering* **134** (8), 1147–1152.

Emiroglu, M. E. & Baylar, A. H. M. E. T. 2003 An investigation of effect of stepped chutes with end sill on aeration performance. *Water Quality Research Journal* **38** (3), 527–539.

Fischer, M. M. 1998 Computational neural networks: a new paradigm for spatial analysis. *Environment and Planning A* **30** (10), 1873–1891.

Gulliver, J. S., Thene, J. R. & Rindels, A. J. 1990 Indexing gas transfer in self-aerated flows. *Journal of Environmental Engineering* **116** (3), 503–523.

Jang, J. S. 1993 ANFIS: adaptive-network-based fuzzy inference system. *IEEE Transactions on Systems, Man, and Cybernetics* **23** (3), 665–685.

Kells, J. A. 1994 Energy dissipation at a gabion weir with through flow and overflow. In *Annual Conference on Canadian Society for Civil Engineering*, pp. 26–35.

Kumar, M., Tiwari, N. K. & Ranjan, S. 2021 Experimental study on oxygen mass transfer characteristics by plunging hollow jets. *Arabian Journal for Science and Engineering* **46** (5), 4521–4532.

Kumar, M., Tiwari, N. K. & Ranjan, S. 2022 Soft computing based predictive modelling of oxygen transfer performance of plunging hollow jets. *ISH Journal of Hydraulic Engineering* **28** (suppl 1), 223–233.

Lewis, W. K. & Whitman, W. G. 1924 Principles of gas absorption. *Industrial & Engineering Chemistry* **16** (12), 1215–1220.

Luxmi, K. M., Tiwari, N. K. & Ranjan, S. 2022 Application of soft computing approaches to predict gabion weir oxygen aeration efficiency. *ISH Journal of Hydraulic Engineering* 1–15. https://doi.org/10.1080/09715010.2022.2050311.

Markofsky, M. & Kobus, H. 1978 Unified presentation of weir-aeration data. *Journal of the Hydraulics Division* **104** (4), 562–568.

Nigrin, A. 1993 *Neural Networks for Pattern Recognition*. MIT Press, Cambridge, MA and London, UK.

Peyras, L. A., Royet, P. & Degoutte, G. 1992 Flow and energy dissipation over stepped gabion weirs. *Journal of Hydraulic Engineering* **118** (5), 707–717.

Raikar, R. V. & Kamatagi, P. B. 2015 Use of hydraulic phenomena in enhancement of dissolved oxygen concentration. *International Journal of Research in Engineering Technology* **4** (2), 568–574.

Salmasi, F., Chamani, M. R. & Farsadi, Z. D. 2012 Experimental study of energy dissipation over stepped gabion spillways with low heights. *Iranian Journal of Science and Technology Transactions of Civil Engineering* **36** (C2), 253–264.

Sharafati, A., Yasa, R. & Azamathulla, H. M. 2018 Assessment of stochastic approaches in prediction of wave-induced pipeline scour depth. *Journal of Pipeline Systems Engineering and Practice* **9** (4), 04018024.

Sharafati, A., Haghbin, M., Aldlemy, M. S., Mussa, M. H., Ahmed, W., Al Zand, A. M., Bhagat, S. K., Al-Ansari, N. & Yaseen, Z. M. 2020a Development of advanced computer aid model for shear strength of concrete slender beam prediction. *Applied Sciences* **10** (11), 3811.

Sharafati, A., Tafarojnoruz, A., Shourian, M. & Yaseen, Z. M. 2020b Simulation of the depth scouring downstream sluice gate: the validation of newly developed data-intelligent models. *Journal of Hydro-Environment Research* **29**, 20–30.

Singh, A., Singh, B. & Sihag, P. 2021 Experimental investigation and modeling of aeration efficiency at labyrinth weirs. *Journal of Soft Computing in Civil Engineering* **5** (3), 15–31.

Tiwari, N. K. 2021 Evaluating hydraulic jump oxygen aeration by experimental observations and data driven techniques. *ISH Journal of Hydraulic Engineering* **27** (suppl 1), 601–615.

Tiwari, N. K. & Sihag, P. 2020 Prediction of oxygen transfer at modified Parshall flumes using regression models. *ISH Journal of Hydraulic Engineering* **26** (2), 209–220.

Verma, A., Ranjan, S., Ghanekar, U. & Tiwari, N. K. 2022 Soft computing techniques for predicting aeration efficiency of gabion stepped weir. In: J. P. Davin, ed. *Proceedings of the International Conference on Industrial and Manufacturing Systems (CIMS-2020)*. Springer, Cham, pp. 117–122.

Wormleaton, P. R. & Soufiani, E. 1998 Aeration performance of triangular planform labyrinth weirs. *Journal of Environmental Engineering* **124** (8), 709–719.

Wuthrich, D. & Chanson, H. 2015 Aeration performances of a gabion stepped weir with and without capping. *Environmental Fluid Mechanics* **15** (4), 711–730. doi:10.1007/s10652-014-9377-9.

Zhang, G. & Chanson, H. 2016 Hydraulics of the developing flow region of stepped spillways. I: Physical modeling and boundary layer development. *Journal of Hydraulic Engineering* **142** (7), 1–8. doi:10.1061/(ASCE)HY.1943-7900.0001138.